














ORIGINAL RESEARCH

An mTORC1-Dependent Mouse Model for Cardiac Sarcoidosis

Carlos Bueno-Beti , PhD*; Clarice X. Lim , PhD*; Alexandros Protonotarios , MD; Petra Lujza Szabo , PhD; Joseph Westaby , MD; Mario Mazic , Msc; Mary N. Sheppard , MD; Elijah Behr , MD; Ouafa Hamza , MD PhD; Attila Kiss, PhD; Bruno K. Podesser , MD; Markus Hengstschläger , PhD; Thomas Weichhart , PhD; Angeliki Asimaki , PhD

BACKGROUND: Sarcoidosis is an inflammatory, granulomatous disease of unknown cause affecting multiple organs, including the heart. Untreated, unresolved granulomatous inflammation can lead to cardiac fibrosis, arrhythmias, and eventually heart failure. Here we characterize the cardiac phenotype of mice with chronic activation of mammalian target of rapamycin (mTOR) complex 1 signaling in myeloid cells known to cause spontaneous pulmonary sarcoid-like granulomas.

METHODS AND RESULTS: The cardiac phenotype of mice with conditional deletion of the *tuberous sclerosis 2 (TSC2)* gene in CD11c⁺ cells (*TSC2^{fl/fl}CD11c-Cre*; termed *TSC2^{KO}*) and controls (*TSC2^{fl/fl}*) was determined by histological and immunological stains. Transthoracic echocardiography and invasive hemodynamic measurements were performed to assess myocardial function. *TSC2^{KO}* animals were treated with either everolimus, an mTOR inhibitor, or Bay11-7082, a nuclear factor-κB inhibitor. Activation of mTOR signaling was evaluated on myocardial samples from sudden cardiac death victims with a postmortem diagnosis of cardiac sarcoidosis. Chronic activation of mTORC1 signaling in CD11c⁺ cells was sufficient to initiate progressive accumulation of granulomatous infiltrates in the heart, which was associated with increased fibrosis, impaired cardiac function, decreased plakoglobin expression, and abnormal connexin 43 distribution, a substrate for life-threatening arrhythmias. Mice treated with the mTOR inhibitor everolimus resolved granulomatous infiltrates, prevented fibrosis, and improved cardiac dysfunction. In line, activation of mTOR signaling in CD68⁺ macrophages was detected in the hearts of sudden cardiac death victims who suffered from cardiac sarcoidosis.

CONCLUSIONS: To our best knowledge this is the first animal model of cardiac sarcoidosis that recapitulates major pathological hallmarks of human disease. mTOR inhibition may be a therapeutic option for patients with cardiac sarcoidosis.

Key Words: cardiac sarcoidosis ■ fibrosis ■ heart ■ mouse model ■ mTORC1 ■ sarcoidosis

Sarcoidosis is a systemic inflammatory disease that is histologically characterized by the formation and accumulation of non-necrotizing granulomas, primarily in the lungs, but can also manifest independently in other organs such as the heart.^{1,2} Particularly during cardiac sarcoidosis (CS), unresolved granulomatous inflammation is life-threatening when diagnosed late and untreated and can eventually

lead to cardiac fibrosis, arrhythmias, and sudden cardiac death.³ Clinically apparent cardiac sarcoidosis has been reported in 5% to 7% of the patients with systemic sarcoidosis and is associated with a poor outcome.⁴ However, based on postmortem evaluation, cardiac involvement of sarcoidosis has been reported in 25% to 58% of the patients.⁵ In the Japanese population, cardiac involvement is the leading cause of

Correspondence to: Thomas Weichhart, PhD, Center for Pathobiochemistry and Genetics, Medical University of Vienna, Währingerstraße 10, 1090 Vienna, Austria. Email: thomas.weichhart@meduniwien.ac.at and Angeliki Asimaki, PhD, Clinical Cardiology Academic Group, St. George's, University of London, Corridor 10, 1st floor Jenner Wing, Cranmer Terrace, SW17 0RE London, United Kingdom. Email: aasimaki@sgul.ac.uk

*C. Bueno-Beti and C. X. Lim contributed equally.

This manuscript was sent to Rebecca D. Levit, MD, Associate Editor, for review by expert referees, editorial decision, and final disposition.

Supplemental Material is available at <https://www.ahajournals.org/doi/suppl/10.1161/JAHA.123.030478>

For Sources of Funding and Disclosures, see page 12.

© 2023 The Authors. Published on behalf of the American Heart Association, Inc., by Wiley. This is an open access article under the terms of the [Creative Commons Attribution-NonCommercial-NoDerivs](https://creativecommons.org/licenses/by-nc-nd/4.0/) License, which permits use and distribution in any medium, provided the original work is properly cited, the use is non-commercial and no modifications or adaptations are made.

JAHA is available at: www.ahajournals.org/journal/jaha

RESEARCH PERSPECTIVE

What Is New?

- Constitutive activation of mammalian target of rapamycin complex 1 signaling in CD11c-expressing cells in mice promotes cardiac granuloma formation, recapitulating several features of human cardiac sarcoidosis including inflammatory granulomatous infiltration, gap junction remodeling, progressive interstitial, perivascular fibrosis, and diastolic dysfunction with preserved ejection fraction.
- Mammalian target of rapamycin inhibition with everolimus reduces inflammatory infiltration and cardiac fibrosis, reverses gap junction remodeling, and improves cardiac function in this sarcoidosis model.

What Question Should Be Addressed Next?

- Because 78% of sudden cardiac death victims with a postmortem diagnosis of cardiac sarcoidosis stain positive for mammalian target of rapamycin complex 1 activation, our findings indicate the use of mammalian target of rapamycin inhibitors as potential therapeutic option for patients with cardiac sarcoidosis and suggest the use of p-S6 as marker for the diagnosis of high-risk (poor prognosis) patients.

Nonstandard Abbreviations and Acronyms

ACM	arrhythmogenic cardiomyopathy
CS	cardiac sarcoidosis
mTORC1	mTOR complex 1
mTOR	mammalian target of rapamycin
MHC	major histocompatibility complex
NF-kB	nuclear factor k-light-chain-enhancer of activated B cells
TSC2	tuberous sclerosis complex 2

death related to sarcoidosis, accounting for up to 85% of deaths.⁶

Often referred to as the great mimicker, sarcoidosis is a diagnosis of exclusion⁷ and shares histopathological and clinical phenotype with arrhythmogenic cardiomyopathy (ACM).⁸ Abnormal distribution of plakoglobin, a cytoplasmic structural component of the desmosome, and connexin 43, the main ventricular gap junction protein, at the intercalated disks is a key feature of ACM and sarcoidosis and an indicator of early disease progression.^{9,10} Recently, nuclear factor k-light-chain-enhancer of activated B cells (NF-kB)

induced inflammation has been proposed as a driver of the key pathological features of ACM, and its inhibition with BAY11-7082 prevents the development of the disease features in a range of in vitro, in vivo, and ex vivo models of ACM.¹¹

Although environmental, genetic, and microbial factors have been postulated to underlie sarcoidosis, its pathogenesis remains unknown. Consequently, glucocorticoids continue to be the first-line management option.^{12,13} For patients with refractory CS, a stepwise approach, including steroid-sparing alternatives and monoclonal antibodies, has been proposed, but randomized controlled studies to systematically evaluate the efficacy of these drugs are lacking.⁷ There is a pressing need to develop mechanism-based therapies to treat CS. The development of experimental models that recapitulate the process of granuloma formation in the heart would allow for mechanistic insights into the molecular events underlying the disease and suggest novel therapeutic targets. To date, no experimental models of sarcoidosis with cardiac involvement have been reported.¹⁴

We previously showed that genetic deletion of tuberous sclerosis complex 2 (*TSC2*) in myeloid lineage *Lyz2* expressing cells (targeting monocytes, macrophages, and granulocytes) led to spontaneous development of pulmonary sarcoid-like granulomas in mice.¹⁵ Exome sequencing studies have also implicated genes coding for regulators of mammalian target of rapamycin (mTOR) and autophagy in familial forms of sarcoidosis.¹⁶ Here we phenotyped the heart of mice with conditional genetic deletion of *TSC2* (an upstream inhibitor of mTOR complex 1 [mTORC1]) in CD11c-expressing cells, where we also found spontaneous development of sarcoid-like granulomas in the lungs. The aims of this study were (1) to characterize cardiac involvement in the *TSC2^{fl/fl}*CD11c-Cre model of sarcoidosis, and (2) to evaluate the efficacy of 2 mechanism-based therapies: everolimus (targeting the mTOR signaling pathway) and BAY11-7082 (inhibiting the NF-kB pathway).

METHODS

All data and supporting materials have been provided within the published article.

Animal Model

In this study we used a mouse model of sarcoidosis with mTORC1 constitutive expression in CD11c-expressing cells generated by deleting its upstream inhibitor *TSC2*. In brief, *TSC2^{fl/fl}* mice¹⁷ were crossed with transgenic mice expressing Cre recombinase under the control of the CD11c promoter, CD11c-Cre mice.¹⁸ Both male and female mice between 13 and 54 weeks old were used. All mouse studies were approved by the official

Austrian ethics committee for animal experiments (GZ.BMWF-66.009/0163-WF/V/3b/2016 and BMBWF GZ-2021-0.611.635).

In Vivo Treatments

Male and female *TSC2^{fl/fl}* CD11c-Cre (*TSC2^{KO}*) mice, already displaying symptoms at 26 weeks of age were treated by oral gavage with 5 mg/kg body weight everolimus (RAD001, Selleckchem) or diluent (PBS with 0.05% DMSO, 30% PEG [Sigma 202371], 5% Tween-80 [Sigma P1754-25 mL]) daily for 3 and 21 days. To study the role of NF- κ B signaling in the disease progression, another group of *TSC2^{KO}* mice were injected intraperitoneally with 5 mg/kg Bay11-7082 (Sigma 196870) or vehicle (5% DMSO/saline) every day for 21 days. The drug and the vehicle were administered to both males and females between 24 to 26 weeks of age. At this dose, Bay11-7082 has been shown to block NF- κ B signaling in several in vivo studies. Age-matched *TSC2^{fl/fl}* littermates were used as controls.

Histology and Immunohistochemistry of Heart Samples

Mouse hearts were fixed in ROTI Histofix 4% formaldehyde (Carl Roth), processed, and embedded in paraffin. Tissue morphology and the presence of inflammatory cells were evaluated by conventional hematoxylin and eosin staining and tissue fibrosis by picosirius red staining. Whole heart sections from mice were stained and bright field images taken with a Nikon eclipse 80i microscope and recorded with a Nikon DS-Fi1 camera. Protein expression and localization on mouse myocardial tissue samples were evaluated by confocal immunofluorescence. In brief, 5 μ m heart sections were deparaffinized and rehydrated. Following citrate antigen retrieval, slides were incubated overnight at 4 °C with primary antibodies: anti-Galectin 3 (Mac-2) (Abcam, ab76245 or Cedarlane CL8942AP), rabbit monoclonal anti-Phospho-S6 Ribosomal Protein (p-S6) (Ser240/244) (Cell Signaling Technology, 5364S), rabbit polyclonal anti-N-Cadherin (Merck, C3678), rabbit monoclonal anti-gamma Catenin (plakoglobin) (Abcam, ab184919), rabbit polyclonal anti-Connexin 43 (Merck, C6219), rabbit monoclonal anti-CD3 (Abcam, ab5690), CD206 polyclonal antibody (Thermo Fisher PA5-46994), or rat anti-CD68 (Thermo Fisher, 14-0681-82). The next day, heart sections were incubated with host-specific Cy3-conjugated secondary antibodies and mounted with ProLong Gold (Invitrogen, P36935). Immunoreactive signal was recorded by either Nikon A1R confocal microscope or Zeiss Axioscan 7. Collagen content (fibrosis) in mouse heart sections was quantified as described by Vogel et al¹⁹ and expressed as % of total tissue area. For image quantification, 5 microscopy fields were analyzed per

preparation. Fluorescence image analysis was performed with Zen Blue 3.4 software (Zeiss).

Human Cardiac Sarcoidosis Samples

Human heart samples from 9 sudden cardiac death victims with a definite postmortem diagnosis of CS by an expert cardiac pathologist were obtained from the Cardiac Risk in the Young Centre for Cardiac Pathology at St. George's, University of London. Ethical approval for this study was granted by the London Stanmore National Health Service Research Ethics Committee (reference: 17/LO/0747). Informed consent was provided by next-of-kin at the time of autopsy. Heart tissue sections from the right ventricle (RV), left ventricle (LV), and interventricular septum from paraformaldehyde-fixed paraffin-embedded heart samples were immunostained with rabbit monoclonal anti-CD68 (Abcam, ab213363), rat monoclonal anti-mouse/human Mac-2 (Cedarlane CL8942AP), or rabbit monoclonal anti-Phospho-S6 Ribosomal Protein (p-S6) (Ser240/244) antibodies. Immunoreactive signal was recorded with Nikon A1R confocal microscope.

Echocardiography

Transthoracic echocardiography was performed using a Vevo 3100 Imaging system (Visualsonics) with a 55-MHz transducer as described previously.²⁰ The mice (aged 26–29 weeks of age) were anesthetized with 1% to 1.5% isoflurane. Body temperature and ECG were continuously monitored throughout the measurement via limb electrodes and rectal probe, respectively. Parasternal long-axis view and short axis view were obtained, which were analyzed to assess the LV dimension and function. The obtained ultrasound images and videos were analyzed by Vevo LAB software where a mean of 3 cardiac cycles in each view was used for each parameter.

Hemodynamic Measurements

Mice at 26 to 29 weeks of age were anesthetized with a mixture of ketamine and xylazine, trachea cannulated, and the mice were mechanically ventilated. When the ECG was stable, the thorax was opened and a microtip catheter (Millar Instruments) was inserted first in the LV then into the RV to monitor the hemodynamic parameters at least for 10 minutes with Powerlab system with LabChart (v7.3.2) software (ADInstruments) as described previously.²⁰

Statistical Analysis

Statistical analysis was performed using Prism software (Version 9.2.0 [283]; GraphPad Software Inc., San Diego, CA). Normality distribution of the data was assessed by Kolmogorov–Smirnov test. Data were

analyzed for differences by using a Mann–Whitney test for single comparison, 1-way analysis of variance (ANOVA) and the Newman–Keuls post-test for multiple comparisons, Kruskal–Wallis test with Dunn post hoc (Bonferroni) multiple comparison test, and 2-way ANOVA and the Tukey post-test for multiple comparison. Data in the text and figures are presented as mean \pm SEM. *P* values <0.05 were considered significant.

RESULTS

Granulomatous Disease in the Hearts of Mice With Constitutive Activation of mTORC1 in CD11c-Expressing Myeloid Cells

Similar to our observations in the *TSC2^{fl/fl}* Lyz2-Cre mouse model¹⁵ where we found spontaneous development of pulmonary sarcoid-like granulomas after genetic ablation of *TSC2* in Lyz2 expressing myeloid cells, constitutive activation of mTORC1 by deletion of *TSC2* in CD11c-expressing cells termed *TSC2^{KO}* (affecting tissue resident macrophages and dendritic cells) was also sufficient to initiate and maintain granulomas in the lung (Figure S1). In addition, *TSC2^{KO}* mice showed slightly elevated tumor necrosis factor- α levels in the serum compared with their littermate controls (Figure S1D).

Histological investigation of the hearts of adult *TSC2^{KO}* animals revealed the presence of a significantly higher number of inflammatory cells in the base and midventricular areas of the left ventricular free wall, interventricular septum, RV, LV, papillary muscles, and to a lesser extent in the atria and visceral pericardium (Figure 1A; Figures S2 and S3). Increased inflammatory infiltration of the mitral and tricuspid valves was also observed in the *TSC2^{KO}* sarcoidosis mice (Figure S3). Inflammatory cells were mainly distributed between cardiomyocytes (interstitial) and around the blood vessels (perivascular) (Figure 1A) and consisted mostly of activated Mac-2⁺ macrophages expressing CD68 and CD206 (Figure 1B; Figures S2 and S3). Some animals showed structures reminiscent of giant cells and non-necrotizing granulomas (Figure 1C) as observed in human patient hearts.²¹ Few T lymphocytes (CD3⁺ cells) were observed in the hearts of the *TSC2^{KO}* animals (Figure 1D). Here, the presence of inflammatory infiltrates was associated with myocardial damage and increased interstitial and perivascular fibrosis (Figure 1E).

Progressive Granulomatous Disease and Fibrosis Over Time

Progressive and chronic sarcoidosis, unlike Löfgren syndrome sarcoidosis, is unlikely to resolve spontaneously

with time, and such patients are also more likely to be refractory to corticosteroid treatment.²² To investigate if cardiac disease seen in these mice is chronic and progresses over time, we measured the number of Mac-2⁺ macrophages, the activation of mTORC1 signaling pathway, and the amount of fibrosis in the hearts of control and *TSC2^{KO}* mice at 13 and 54 weeks of age (Figure S2D).

At 13 weeks of age, we observed the presence of few Mac-2⁺ cells in the pericardium, the perivascular, and interstitial areas of the myocardium of the *TSC2^{KO}* animals. At 54 weeks of age, the area occupied by Mac-2⁺ cells in the hearts of *TSC2^{KO}* animals increased from 0.43% \pm 0.12% to 5.58% \pm 0.75% (*P* <0.0001). Mac-2⁺ cells were absent in the hearts of control animals at 13 and 54 weeks of age (Figure 2B). To evaluate mTORC1 signaling pathway involvement in the progression of the granulomatous infiltration in the hearts of the *TSC2^{KO}* animals, we measured the phosphorylation of the downstream effector ribosomal protein S6 (p-S6), a hallmark of mTORC1 activation (Figure 2C). Phosphorylation levels of S6, as determined by the percentage of area occupied by cells expressing p-S6, increased from 0.446% \pm 0.067% in the *TSC2^{KO}* animals at 13 weeks of age to 4.54% \pm 0.39% in the *TSC2^{KO}* animals at 54 weeks of age (*P* <0.0001 ; Figure 2D). The expression of p-S6 was virtually absent in the hearts of control mice at 13 and 54 weeks of age.

Increasing accumulation of macrophages with activated mTOR in the hearts of *TSC2^{KO}* animals over time was associated with progressive myocardial destruction and fibrotic replacement (Figure 2E). At 13 weeks of age, we observed a trend toward increased fibrosis in the hearts of *TSC2^{KO}* animals when compared with 13-week-old control mice (Figure 2E and 2F). The percentage of fibrosis in the hearts (RV, LV, and interventricular septum) of *TSC2^{KO}* mice at 54 weeks old was significantly higher than in the control mice at 54 weeks old and 13 weeks old (3.45% \pm 0.026% versus 1.80% \pm 0.15% and 1.92% \pm 0.313%, respectively; *P* <0.01 , Figure 2F).

Gap Junction Remodeling in Hearts of Sarcoidosis Mice

A high proportion of sarcoidosis-related hospitalizations—one-fifth reported in 1 population study²³—involve patients who suffer from arrhythmias, and there are many overlaps in clinical presentation between cardiac sarcoidosis patients and patients with ACM, including a higher risk for sudden cardiac death.^{24,25} Therefore, we analyzed the expression and distribution of the desmosomal protein plakoglobin and connexin 43, the main protein in cardiac

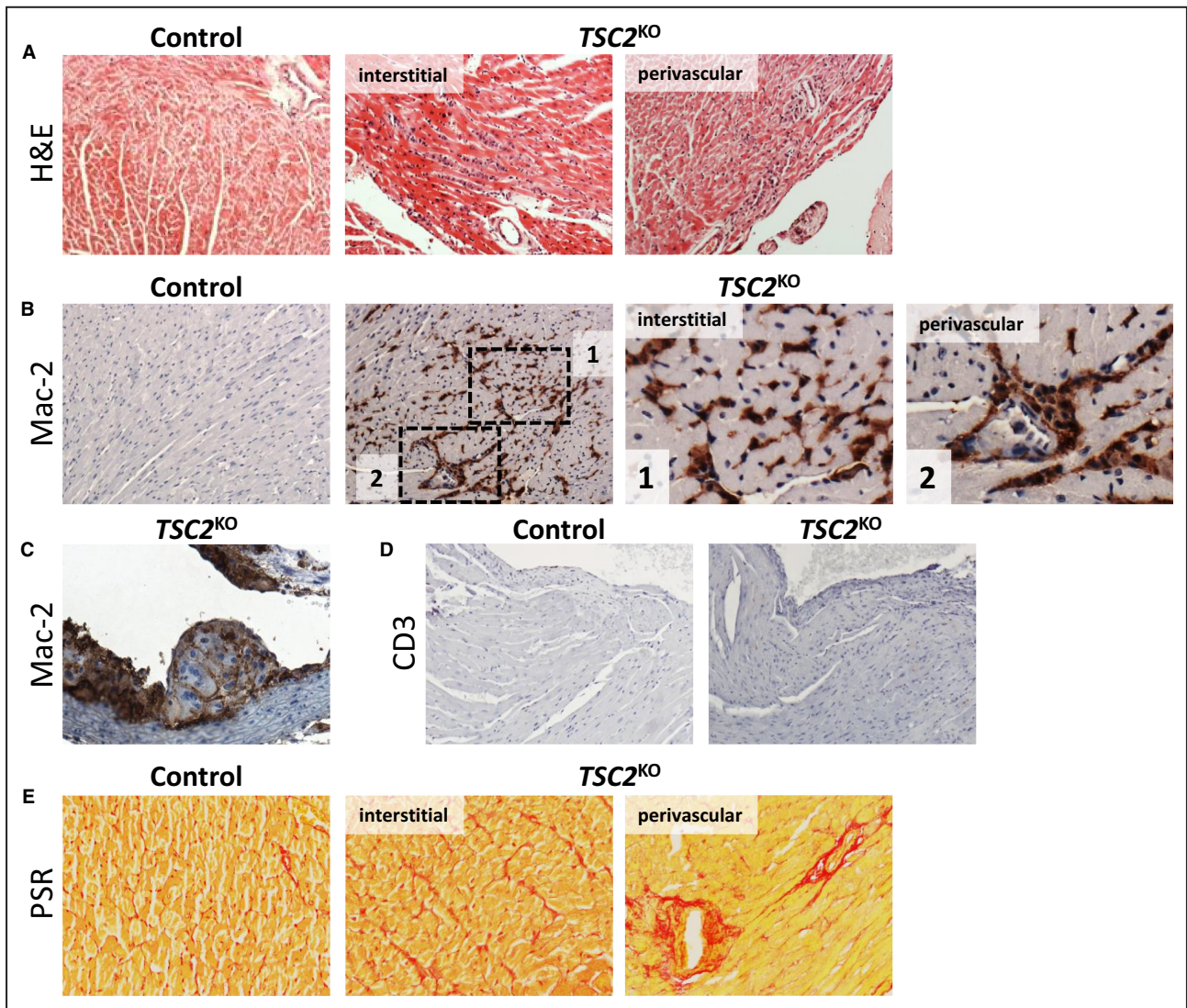


Figure 1. Histopathological characterization of *TSC2^{KO}* mouse hearts at 26 weeks of age.

A, Hematoxylin and eosin staining (200× magnification). Heart sections of *TSC2^{KO}* mice showed increased numbers of inflammatory cells between cardiomyocytes (interstitial) and around the blood vessels (perivascular). **B**, Immunoperoxidase staining with Mac-2 (200× magnification) of control and *TSC2^{KO}* heart section. 1 and 2 are close-up images (600× magnification) showing the presence of interstitial and perivascular Mac-2⁺ cells in the hearts of *TSC2^{KO}* respectively. **C**, Structures reminiscent of human giant cells and non-necrotizing granulomas. **D**, Immunoperoxidase staining CD3 (200× magnification). Inflammatory cells in the hearts of *TSC2^{KO}* mice were mainly Mac-2⁺ cells. **E**, Picosirius red staining (400× magnification). The presence of inflammatory cells in the hearts of *TSC2^{KO}* mice correlated with increased deposition of interstitial and perivascular collagen fibers (n=6 mice/group). H&E indicates hematoxylin and eosin; PSR, picosirius red; and *TSC2^{KO}*, tuberous sclerosis complex 2 knockout.

ventricular gap junctions. The housekeeping protein N-Cadherin was used as a tissue quality control, and its expression levels and distribution pattern were similar between controls and *TSC2^{KO}* animals. Similar to patients with cardiac sarcoidosis and patients with ACM,^{9,26} adult *TSC2^{KO}* mice presented with reduced immunoreactive signal for plakoglobin at the myocardial intercalated disks (Figure 3A). Additionally, heterogeneous connexin 43 remodeling, known to constitute a threatening substrate for fatal

arrhythmias,²⁷ was observed at intercalated disks of *TSC2^{KO}* mice hearts.

***TSC2^{KO}* Sarcoidosis Mice Have Diastolic Dysfunction With Preserved Ejection Fraction**

Despite the presence of inflammatory infiltrates in the hearts of the *TSC2^{KO}* mice, they presented with lighter hearts and decreased heart weight to tibia length ratio

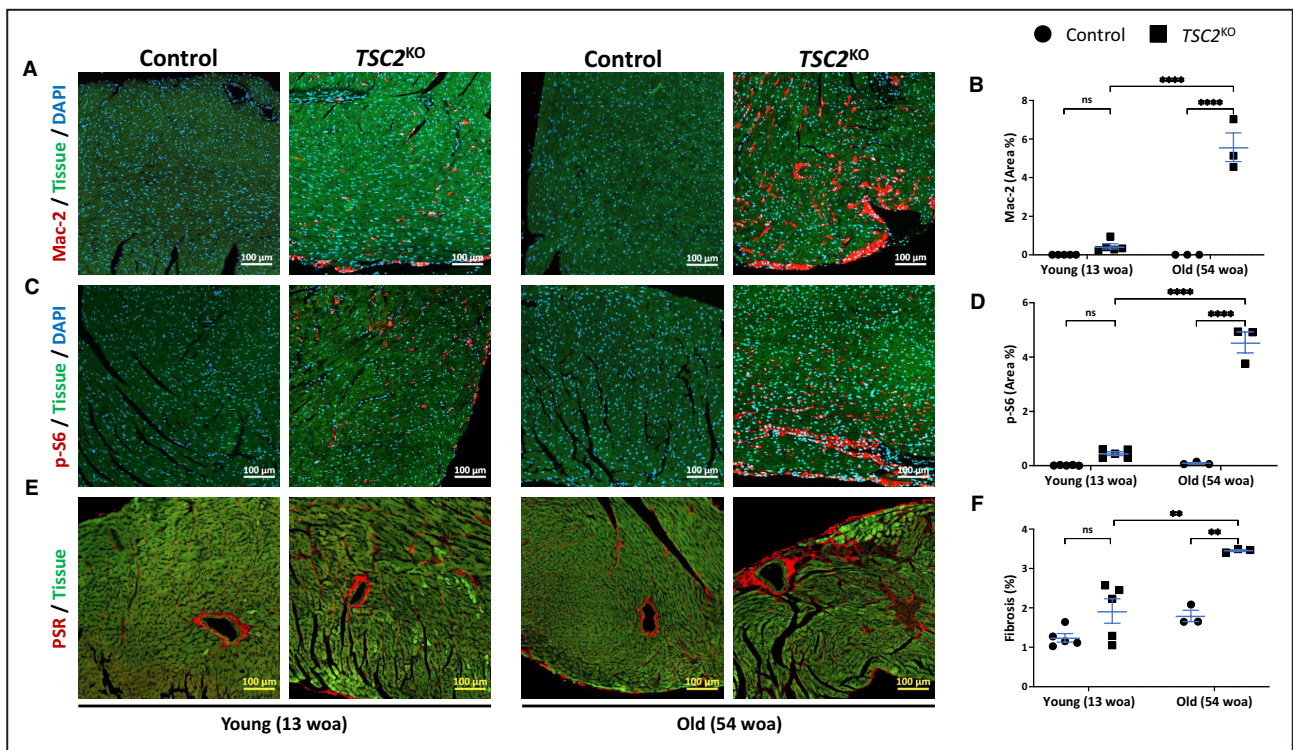


Figure 2. Cardiac involvement is progressive in the *TSC2^{KO}* animal model of sarcoidosis.

A, Confocal images are representative of control and *TSC2^{KO}* mice hearts at 13 and 54 woa immunostained with Mac-2 (red); autofluorescence (green) was used to calculate the area of live cells (total area) in the tissue; nuclei were counterstained with DAPI (blue). **B**, Mac-2 percentage was determined with Zen Blue 3.4 software and was calculated by dividing the area occupied with Mac-2⁺ cells (red) by total tissue area (green). **C**, Representative confocal images of control and *TSC2^{KO}* mice hearts at 13 woa and 54 woa immunostained with p-S6 (red); live cells in the tissue (green); nuclei (blue). **D**, p-S6 percentage was calculated as in **(B)**. **E**, Confocal images representative of control and *TSC2^{KO}* mice hearts at 13 woa and 54 woa stained with picrosirius red. Collagen fibers (red) and area of live cells in the tissue (green). Images were acquired and analyzed as in Vogel et al.¹⁹ **F**, Percentage of fibrosis in the hearts of control and *TSC2^{KO}* animals at 13 woa and 54 woa. Data are expressed as mean±SEM. (n=5/group for 13 woa animals and n=3/group for 54 woa animals). ***P*<0.01 and *****P*<0.0001 by 1-way ANOVA with Tukey multiple comparison test. ns indicates not significant; PSR, picrosirius red; *TSC2^{KO}*, tuberous sclerosis complex 2 knockout; and woa, weeks of age.

(Figure 3B) compared with control *TSC2^{fl/fl}* mice. To understand the functional consequences that constitutive activation of mTORC1 signaling in CD11c⁺ cells and Mac-2⁺ macrophage infiltration has on the heart of these mice, we performed echocardiography and hemodynamic pressure measurements on middle-aged mice displaying symptoms between 26 and 29 weeks of age. At this age, the mice already exhibited significant infiltration of Mac-2 inflammatory infiltrates and fibrosis (Figure S4). Although we did not find significant changes in left ventricle ejection fraction or fractional shortening, we saw a decrease in the left ventricular internal diameter in diastole, left ventricular end diastolic volume, left ventricle end systolic pressure, and dP/dt values in the *TSC2^{KO}* mice (Figure 3C). In addition, elevated left ventricle end diastolic pressure and right ventricular end systolic pressure was observed in *TSC2^{KO}* mice in comparison with their controls (Figure 3D).

Bay11-7082 Treatment Ineffective in Reducing Granulomatous Inflammation or Gap Junction Remodeling in Sarcoidosis Mice

Having characterized the sarcoid development in the heart of *TSC2^{KO}* mice, we wanted to assess whether we can therapeutically interfere with the disease. Given the clinical and molecular overlap between sarcoidosis and ACM,⁸ and the recent implication of NF-κB in the pathogenesis of ACM,¹¹ we tested the efficacy of Bay11-7082 in reducing disease-associated features in our model. *TSC2^{KO}* animals between 24 and 26 weeks of age were treated intraperitoneally with 5mg/kg Bay11-7082 or vehicle daily for 21 days. Administration of Bay11-7082 for 21 days was neither able to reduce cardiac (Figure S5A) and pulmonary granulomatous infiltration (not shown) nor inhibit the mTOR signaling pathway (Figure S5B) in the hearts of *TSC2^{KO}*

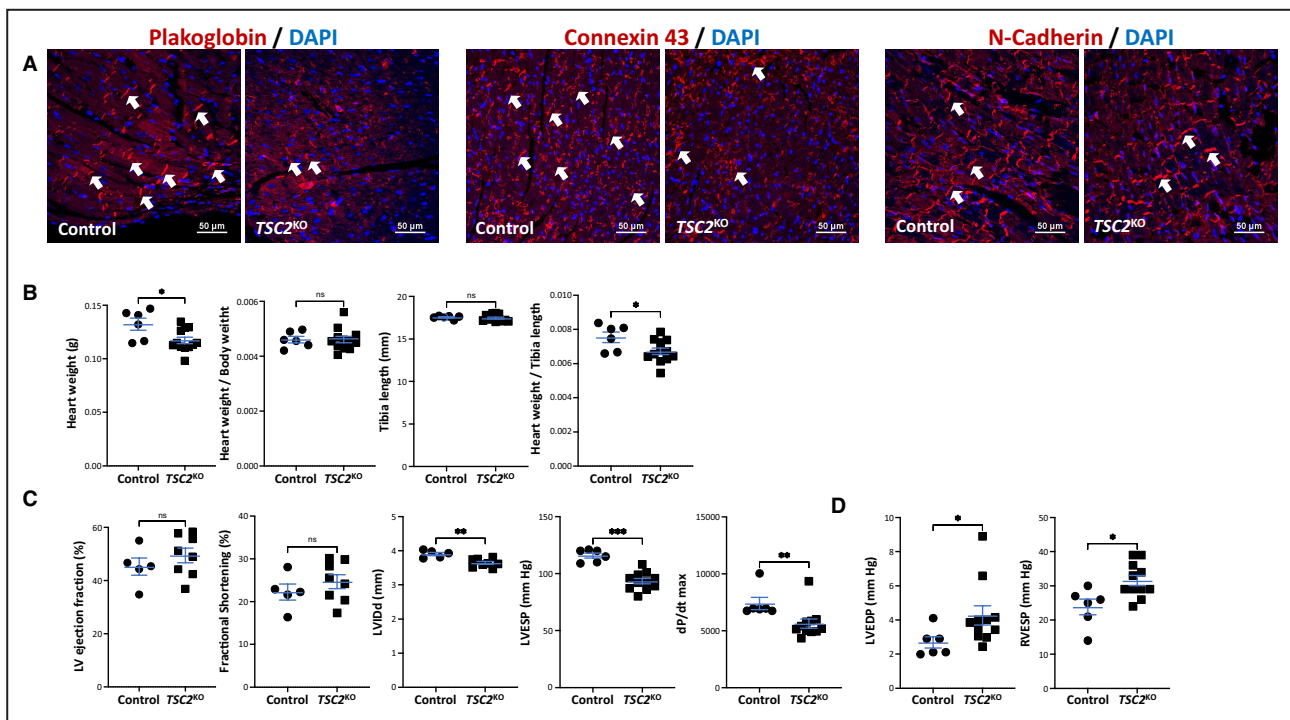


Figure 3. Cardiac phenotype of *TSC2*^{KO} animal model of sarcoidosis.

A, Representative confocal images of control and *TSC2*^{KO} mice hearts immunostained with plakoglobin, connexin 43, and N-Cadherin (red); nuclei were counterstained with DAPI (blue). Arrows show the localization of immunoreactive signal at the intercalated disks. N-cadherin (used as a tissue quality control) shows comparable distribution in both groups. *TSC2*^{KO} animals at 34 weeks of age showed reduced immunoreactive signal for plakoglobin and connexin 43. Scale bar, 50 μm, (n=6/group). **B**, Heart weight, tibia length, body weight, and heart weight to tibia length ratio of control vs *TSC2*^{KO} mice (26–29 weeks of age). **C** through **D**, Quantitative echocardiography and hemodynamic measurements of control and *TSC2*^{KO} mice between 26 to 29 weeks of age. Data are expressed as mean±SEM. **P*<0.05 for controls vs *TSC2*^{KO} by using a Mann–Whitney test. LV indicates left ventricular; LVEDP, left ventricular end diastolic pressure; LVESP, ventricular end systolic pressure; LVIDd, left ventricle internal diameter in diastole; RVESP, right ventricular end systolic pressure; and *TSC2*^{KO}, tuberous sclerosis complex 2 knockout.

animals. In line with these results, expression levels of plakoglobin and connexin 43 were similar between vehicle-treated *TSC2*^{KO} animals and those receiving Bay11-7082 for 21 days (Figure S5C).

mTOR Inhibition Reduces Cardiac Granulomatous Infiltration and Cardiac Fibrosis in Sarcoidosis Model Mice

To test whether mTOR inhibition would improve disease severity, we treated *TSC2*^{KO} animals at 26 weeks of age (already displaying cardiac granulomatous infiltration and fibrosis) by oral gavage with 5 mg/kg body weight¹⁵ with everolimus, an inhibitor of mTOR, or vehicle daily for 3 and 21 days. The 3-day treatment was chosen to evaluate the ability of everolimus to inhibit the phosphorylation of S6,²⁸ whereas the 21-day-treatment regimen was selected to clarify whether administration of the mTOR inhibitor everolimus has therapeutic potential.

Vehicle-treated *TSC2*^{KO} sarcoidosis model mice exhibited 3.14%±0.38% of the heart with granulomatous

Mac-2⁺ cell infiltrates. This percentage was reduced to 1.9%±0.22% (relative 39% reduction) in *TSC2*^{KO} animals receiving everolimus for 3 days (*P* <0.01) and to 0.52%±0.09% (relative 83% reduction) in *TSC2*^{KO} animals receiving everolimus for 21 days (*P*<0.0001) (Figure 4A and 4B). Body weight, heart weight, and tibia length, heart weight to tibia length ratio, and heart rate of the mice were not affected by everolimus treatment (Figure S6A). As expected, everolimus treatment reduced the phosphorylation of the mTOR downstream effector S6 ribosomal protein. The percentage of myocardial tissue occupied by cells expressing p-S6 was reduced by 75% and 95% in *TSC2*^{KO} animals receiving everolimus for 3 and 21 days, respectively (Figure 4C and 4D). In *TSC2*^{KO} animals treated with everolimus for 21 days, the granulomatous infiltrates completely resolved, while they were perfectly recognizable in the hearts of *TSC2*^{KO} animals receiving vehicle. Moreover, everolimus treatment for 21 days was able to halt the progression of fibrotic lesions in the hearts *TSC2*^{KO} animals (Figure 4E and 4F).

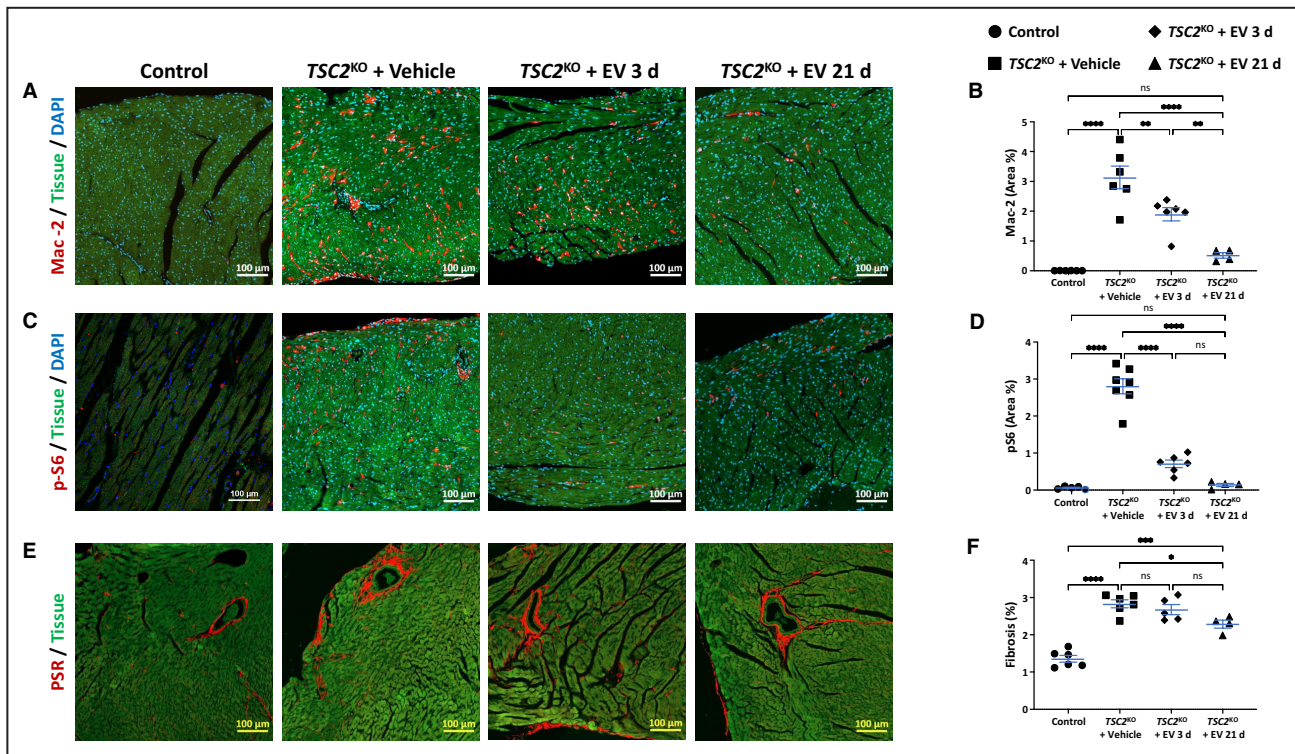


Figure 4. Mammalian target of rapamycin inhibition prevents cardiac sarcoidosis progression in the hearts of *TSC2^{KO}* mice. **A**, Representative confocal images of control and *TSC2^{KO}* mice hearts at 29 weeks of age, treated with everolimus for 3 and 21 days, immunostained with Mac-2 (red); autofluorescence (green) was used to calculate the area of live cells (total area) in the tissue; nuclei were counterstained with DAPI (blue). **B**, Mac-2 percentage was determined with Zen Blue 3.4 software and was calculated by dividing the area occupied with Mac-2+ cells (red) by total tissue area (green). **C**, Representative confocal images of control and *TSC2^{KO}* mice hearts treated as previously described immunostained with p-S6 (red); live cells in the tissue (green); nuclei (blue). **D**, p-S6 percentage was calculated as in **(B)**. **E**, Confocal images are representative of control and *TSC2^{KO}* mice hearts treated with everolimus for 3 and 21 days stained with picrosirius red. Collagen fibers (red); area of live cells in the tissue (green). Images were acquired and analyzed as in Vogel et al.¹⁹ **F**, Percentage of fibrosis in the hearts of control and *TSC2^{KO}* treated as previously described. Data are expressed as mean±SEM. (n=6 for control, *TSC2^{KO}*+vehicle, *TSC2^{KO}*+everolimus 3 days; n=4 for *TSC2^{KO}*+everolimus 21 days). **P*<0.05, ***P*<0.01, ****P*<0.001, and *****P*<0.0001, by 1-way ANOVA with Tukey multiple comparison test. PSR indicates picrosirius red; and *TSC2^{KO}*, tuberous sclerosis complex 2 knockout.

mTOR Inhibition Reverses Gap Junction Remodeling and Improves Cardiac Function in Sarcoidosis Model Mice

Heterogeneous plakoglobin and electrical gap junction remodeling, a substrate for fatal arrhythmias, observed in the vehicle-treated *TSC2^{KO}* animals, was resolved in the *TSC2^{KO}* animals receiving everolimus for 21 days (Figure 5A). Here, we saw that plakoglobin and connexin 43 (Cx43) protein expression levels and their localization at the intercalated disk were reverted to those observed in the control group. Importantly, the echocardiographic and cardiac pressure abnormalities detected in vehicle-treated *TSC2^{KO}* animals, such as reduced left ventricular internal diameter in diastole and left ventricular end diastolic volume and increased LVESP and right ventricular end systolic pressure (Figure 5B and 5C), were normalized to control values in the *TSC2^{KO}* group receiving everolimus for 21 days.

No significant change in left ventricle end diastolic pressure, cardiac dP/dT (max) values, left ventricle internal diameter in systole, left ventricle end systolic volume, left ventricle posterior wall thickness in systole and diastole, or interventricular septum diameter in diastole was observed in the *TSC2^{KO}* mice treated with everolimus (Figure S6B and S6C). Altogether, these results suggest that chronic activation of mTORC1 in CD11c-expressing myeloid cells plays a role in the development of echocardiographic and cardiac pressure abnormalities. Conversely, mTOR inhibition improves cardiac function in this experimental model of sarcoidosis.

mTOR Signaling Pathway Is Active in Human Cardiac Sarcoidosis

Considering that constitutive activation of mTOR signaling in myeloid cells is a sufficient condition for

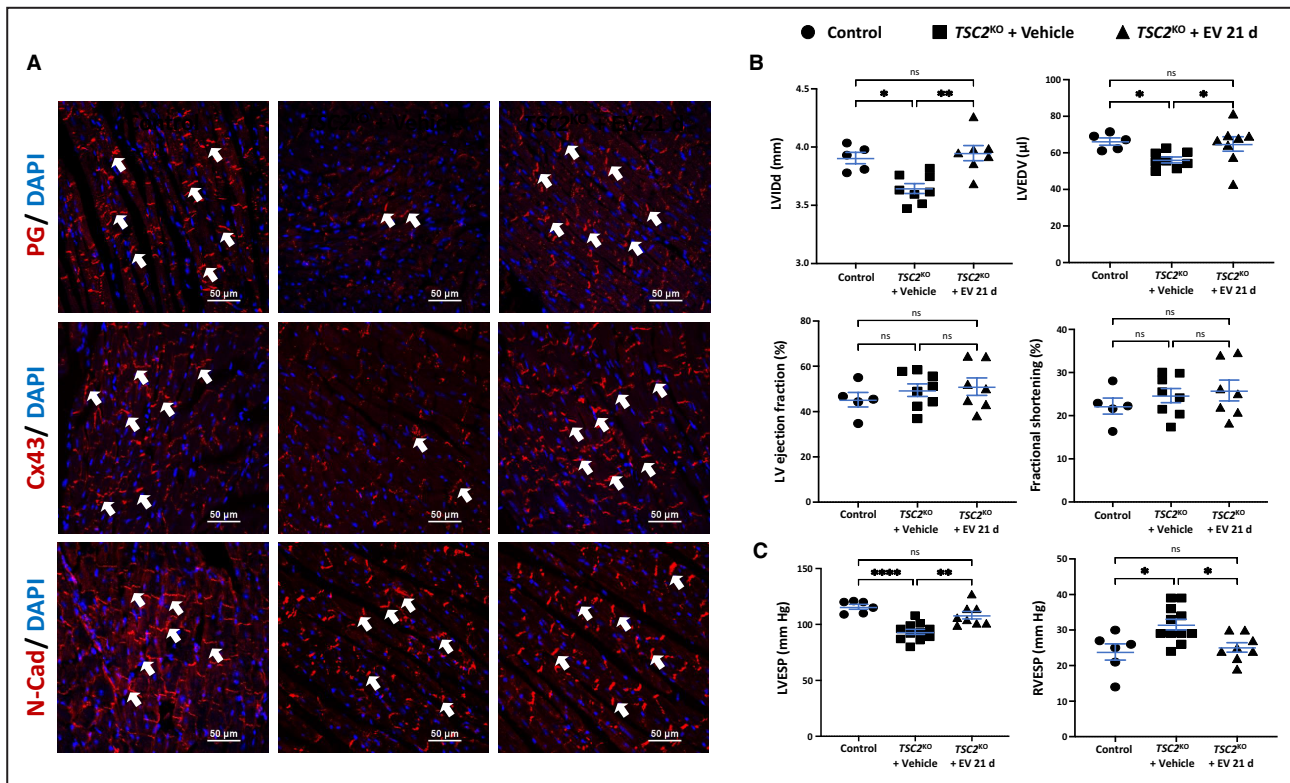


Figure 5. Mammalian target of rapamycin inhibition restores cardiac phenotype and function of the hearts of *TSC2*^{KO} mice. **A**, Representative confocal images of control and *TSC2*^{KO} mice hearts immunostained with N-Cad, plakoglobin, and Cx43 (red); nuclei were counterstained with DAPI (blue). Arrows show the localization of immunoreactive signal at the intercalated disks of the myocardium. N-Cad normal distribution in all experimental groups is shown as a positive control. *TSC2*^{KO} animals showed reduced immunoreactive signal for plakoglobin and Cx43 when compared with the control group. In *TSC2*^{KO} animals receiving everolimus treatment for 21 days, immunoreactive signal for plakoglobin and Cx43 was restored to control levels. Scale bar, 50 μm, (n=4 to 6/group). **B**, Quantitative echocardiography analysis in vehicle- and everolimus-treated *TSC2*^{KO} mice (29 weeks of age) treated for 21 days. Group data for left ventricle internal diameter in diastole, left ventricle end diastolic volume, left ventricular ejection fraction, and fractional shortening. **C**, Hemodynamic pressure measurements of vehicle- and everolimus-treated *TSC2*^{KO} mice treated for 21 days and control mice at 29 weeks of age. Group data showing left ventricular end systolic pressure and right ventricular end systolic pressure. Data are expressed as mean±SEM (n=6 for control group, n=11 for *TSC2*^{KO}+vehicle and n=9 for *TSC2*-knockout+everolimus 21 days). **P*<0.05 and ***P*<0.01, by 1-way ANOVA with Tukey multiple comparison test except for the analysis of left ventricular end diastolic volume where Kruskal–Wallis test with Dunn post hoc (Bonferroni) multiple comparison test was performed. Cx43 indicates connexin 43; LV, left ventricle; LVEDP, left ventricular end diastolic pressure; LVESP, ventricular end systolic pressure; LVIDd, left ventricle internal diameter in diastole; N-Cad, N-Cadherin; RVESP, right ventricular end systolic pressure; and *TSC2*^{KO}, tuberous sclerosis complex 2 knockout.

granulomatous infiltration in the hearts of the *TSC2*^{KO} animals generating a histopathological phenotype highly reminiscent of human CS, we decided to investigate mTOR activation in heart samples from sudden cardiac death victims with a postmortem diagnosis of CS (Figure 6A; Table). We found that non-necrotizing granulomas in the myocardium of patients with CS consisted of CD68⁺ macrophages (Figure 6B). We also found Mac-2 expressing cells among the granulomatous inflammatory infiltrates in the myocardium of the patients (Figure 6C). Additionally, we observed activation of the mTORC1 signaling pathway in 7 out of 9 hearts (78%) of decedents because of CS (Figure 6D; Figure S7). Collectively, these results indicate that mTOR activation may be a relevant mechanism underlying the pathophysiology of human CS.

DISCUSSION

In this study we provide a histopathological and functional description of the first experimental mouse model of progressive systemic sarcoidosis with cardiac involvement. Here we show that constitutive activation of mTORC1 by genetic deletion of *TSC2* in CD11c-expressing myeloid cells led to the presence of inflammatory infiltrates in the hearts of these mice, mainly composed by Mac-2⁺ macrophages, which is associated with increased interstitial and perivascular fibrosis. This is accompanied by gap junction remodeling and diastolic dysfunction with preserved ejection fraction. Therapeutic administration of everolimus, an mTORC1 inhibitor, but not Bay11-7082 was able to rescue the pathological features of CS in this model.

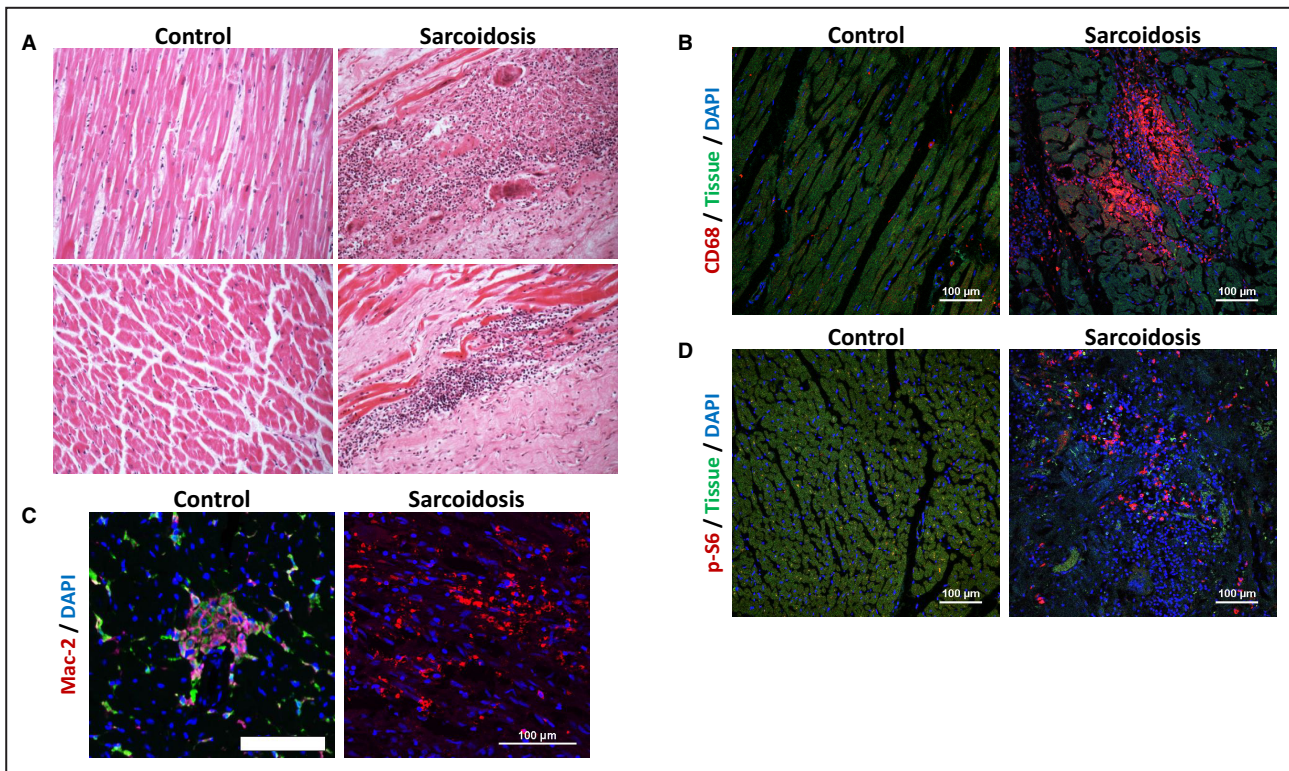


Figure 6. Mammalian target of rapamycin signaling in human cardiac sarcoidosis.

A, Hematoxylin and eosin staining of human heart samples from sudden cardiac death victims with a postmortem diagnosis of cardiac sarcoidosis (200× magnification). **B**, Representative images of hearts immunostained with CD68 and **(C)** Mac-2 and **(D)** p-S6 (red); autofluorescence (green) was used to image healthy myocardial tissue; nuclei were counterstained with DAPI (blue). Images are representative of control subjects (n=6) and patients with cardiac sarcoidosis (n=9). mTOR indicates mammalian target of rapamycin.

Corroborating our mouse model observations, we also show aberrant mTOR activation in myocardial samples of 78% of sudden cardiac death victims with a post-mortem diagnosis of CS.

Table 1. Information on Patients With Sudden Cardiac Death From Which Cardiac Biopsies Were Taken

Patient ID	Age at death, y	Sex	Coexisting conditions	Pathological cause of death
1	33	Male	None	Sarcoidosis
2	33	Male	Tuberculosis	Sarcoidosis
3	54	Male	Obesity	Sarcoidosis
4	36	Male	None	Sarcoidosis, SUDEP
5	53	Male	None	Sarcoidosis
6	44	Male	Obesity	Sarcoidosis
7	47	Female	None	Sarcoidosis
8	41	Male	Fibromyalgia	Sarcoidosis
9	48	Female	Sarcoidosis	Sarcoidosis
	Mean age, y		Male %	
	43.2		77.78	

Age, sex, coexisting diseases, and pathological cause of death are listed. SUDEP indicates sudden unexplained death in epilepsy.

In this mouse model, histological evaluation of the heart revealed the presence of progressive granulomatous infiltrates throughout the myocardium, mostly in the base and midventricular areas of the left ventricle free wall, interventricular septum, and LV and RV. These findings are in line with those reported by Tavora et al in a cohort of patients who died suddenly from CS where the hearts of such patients were characterized by extensive active granulomas, especially in the sub-epicardium and ventricular septum.²⁹ Indeed, old animals (54 weeks of age) with a more severe phenotype also showed structures reminiscent of giant cells and non-necrotizing granulomas. Additionally, we describe a model with cardiac fibrosis that worsens with age. This phenocopies disease progression in CS, where advanced cardiac sarcoidosis correlates with more fibrosis and worse outcomes,³⁰ and the presence of fibrosis is associated with increased disease severity such as congestive heart failure,^{31,32} arrhythmias, and sudden cardiac death.³³

Patients with CS often present with echocardiographic abnormalities, which include dilated cardiomyopathy, diastolic dysfunction, pericardial effusions, and ventricular aneurysms.^{34,35} While the sarcoidosis mice show diastolic dysfunction, reduced left

ventricular ejection fraction, a characteristic criterion used in the diagnosis of CS, was not observed in *TSC2^{KO}* mice that were 26 to 29 weeks of age. Nevertheless, *TSC2^{KO}* animals of this age showed elevation of left ventricle end diastolic pressure and right ventricular systolic pressure. The precise physiological significance of the echocardiographic alterations in the hearts of our sarcoidosis model mice, and its correlation with the echocardiographic abnormalities observed in patients with CS, remain to be determined and will require further investigations. Additionally, the functional significance of mitral and tricuspid valve involvement in these mice needs to be clarified in future studies. Interestingly, CS patients with valve involvement have been reported and deserve further attention in future studies.^{36,37}

Although the cause underlying sarcoidosis still remains elusive, the evidence for a role of aberrant mTOR activation in sarcoidosis is mounting. Previously, we identified rare gene variants encoding for mTOR regulators and autophagy-related proteins in patients with familial sarcoidosis.^{16,13} We also described mTORC1 activation in lung biopsies of patients with progressive sarcoidosis.¹⁵ RNA sequencing of skin lesions from patients with cutaneous sarcoidosis also revealed an enrichment of genes involved in the mTORC1 signaling pathway.^{38,39} Of note, spatial transcriptomics and single nucleus sequencing of frozen cardiac tissues from patients diagnosed with CS revealed the presence of 3 inflammatory macrophage populations, of which 2 populations, the human leukocyte antigen DR isotype (HLA-DR)⁺ and synaptotagmin-like 3 (SYTL3)⁺ macrophage population, show high mTORC1 activation.⁴⁰ Additionally, differentially expressed genes that were upregulated in inflammatory myeloid cells in CS versus resident cardiac macrophages were enriched for the mTOR signaling pathway.⁴⁰ This is in accordance with the observations in our mouse model, where the hearts of control *TSC^{fl/fl}* mice with resident cells and little/no inflammatory infiltrates do not stain positive for p-S6 (mTORC1 activation), while the sarcoidosis model mice show increased activation of mTORC1 and inflammatory infiltration over time, corresponding to disease severity. Moreover, we show that the mTOR signaling pathway was active in the hearts of 78% of sudden cardiac death victims attributable to CS. The specificity of the mTOR findings needs to be examined in the hearts of sudden cardiac death attributable to other pathologies and will be the topic of future investigations. Nevertheless, our results suggest the use of p-S6 or other molecules indicating activated mTORC1 signaling as a target for diagnosis of high-risk CS by routine immunohistochemical staining and for development of tracers for noninvasive molecular imaging as an alternative to current use of echocardiographic measurements, where echocardiographic

abnormalities are often nonspecific and hinder an accurate diagnosis of the disease.⁴¹

Although CD11c is a common marker for dendritic cells, it is also expressed by tissue macrophage populations. In the myocardium, CD11c is highly expressed on mouse CCR2⁺ MHCII high macrophages and lowly expressed on CCR2-MHCII high and low macrophages and Ly6C⁺ macrophages.⁴² In humans, the abundance of CCR2⁺ macrophage population is associated with persistent left ventricular systolic dysfunction after mechanical unloading in patients with heart failure.⁴³ It remains to be seen what role the various macrophages play in CS pathophysiology and if a particular dendritic cell or macrophage population is responsible for the associated phenotypes such as cardiac fibrosis and diastolic dysfunction. However, it is clear that constitutive activation of mTOR signaling in CD11c-expressing cells is able to initiate a CS-like phenotype. Future work should characterize the mTOR high Mac-2⁺ CD11c-expressing cells in this mouse model and clarify their role in disease progression (whether they play a direct or indirect role). Additionally, it would be interesting to compare the macrophages in this model to the 3 inflammatory macrophage populations identified in human CS.⁴⁰

Abnormal plakoglobin and connexin 43 distribution in the myocardium is a shared feature of sarcoidosis and ACM.^{9,44} The latter abnormality, also known as gap junction remodeling, is present in many other cardiomyopathies and is recognized to be a substrate for fatal arrhythmias.⁹ While we show reduced plakoglobin expression and abnormal distribution of connexin 43 in our mouse model as in myocardial samples of patients with CS,⁹ the arrhythmogenic phenotype in this model remains to be determined. ECG monitoring of the mice should be done in future studies to characterize the role of gap junction remodeling on the cardiac conduction system in this mouse model. Previously, a mouse model of ACM showed aberrant activation of NF- κ B, and the treatment with Bay11-7082, an inhibitor of NF- κ B, abolished all disease-associated features.¹¹ The clinical and molecular overlap between ACM and sarcoidosis prompted us to test the efficacy of Bay11-7082 in preventing disease-associated abnormalities in *TSC2^{KO}* animals. Interestingly, treatment with Bay11-7082 neither prevented granulomatous infiltration nor inhibited the mTOR signaling pathway in the hearts of *TSC2^{KO}* animals. However, Bay11-7082 reverses localization of plakoglobin and connexin 43 in an animal model of ACM.¹¹ The fact that Bay11-7082 does not restore physiological distribution of the plakoglobin and connexin 43 proteins in the *TSC2^{KO}* animal model of sarcoidosis implicates disparate pathogenetic mechanisms underlying protein remodeling in these diseases. In prostate cancer, Dan et al indicated that mTOR can control NF- κ B activity via interaction

with and stimulation of IKK.⁴⁵ In fact, more recently, Dai et al showed that in macrophages mTOR deficiency suppresses NF- κ B activation induced by high glucose.⁴⁶ Altogether, this evidence suggests that mTOR is upstream of NF- κ B. Consequently, targeting NF- κ B alone may not be sufficient for prevention of the CS phenotype in our animal model.

In this study we show that therapeutic administration of the mTOR inhibitor everolimus is sufficient to resolve granulomatous infiltrates and prevent the progression of fibrotic lesions in the hearts of *TSC2*^{KO} animals. These changes were associated with the improvement of cardiac dysfunction in *TSC2*^{KO} animals. In agreement with our findings, the administration of sirolimus to a patient with de novo systemic sarcoidosis following a liver transplant resulted in disease resolution.⁴⁷ Similarly, sirolimus was recently used to successfully treat a patient with pulmonary sarcoidosis.⁴⁸ mTOR inhibition was also shown to inhibit pulmonary fibrosis by regulating epithelial-mesenchymal transition⁴⁹ and that targeted inhibition of PI3K/mTOR in lung fibroblasts suppresses pulmonary fibrosis.⁵⁰ Future work should clarify the role played by CD11c-expressing macrophages or cells in the development of fibrosis in CS and their interactions with cardiac fibroblasts.

Altogether, we show that macrophages showing high mTORC1 signaling play an important role in the development and progression of CS. We also present the first animal model of sarcoidosis with cardiac involvement, recapitulating several histopathological features of human CS. This model of CS, though systemic (also affecting the lungs and skin), can be used as a preclinical model to test the efficacy of corticosteroid-sparing alternative drugs and gain insight into the molecular mechanism behind their action. As everolimus treatment clears inflammatory infiltrates and improves cardiac function and fibrosis in this model of sarcoidosis, we propose the use of mTOR inhibitors in future clinical trials to test for efficacy in CS.

ARTICLE INFORMATION

Received June 22, 2023; accepted August 15, 2023.

Affiliations

Clinical Cardiology Academic Group, Molecular and Clinical Research Science Institute, St George's University of London, London, United Kingdom (C.B.-B., J.W., M.N.S., E.B., A.A.); Center for Pathobiochemistry and Genetics, Medical University of Vienna, Vienna, Austria (C.X.L., M.M., M.H., T.W.); Institute of Cardiovascular Science, Clinical Science Research Group, University College London, London, United Kingdom (A.P.); and Center for Biomedical Research, Medical University of Vienna, Vienna, Austria (P.L.S., O.H., A.K., B.K.P.).

Sources of Funding

The authors thank the British Heart Foundation project grant (PG/18/27/33616) for funding all studies related to this project. A. Asimaki is also funded by the Wellcome Trust project grant (208460/Z/17/Z) and Rosetrees Foundation Trust corn seed fund (M689). C. Bueno-Beti is supported by the British Heart Foundation project grant (PG/18/27/33616). Research in the Weichhart

laboratory is supported by funding from the Austrian Science Fund (FWF) grants P34023-B, P34266-B, FWF Sonderforschungsbereich F83, Vienna Science and Technology Fund (WWTF) grant LS18-058, and the Ann Theodore Foundation Breakthrough Sarcoidosis Initiative. Dr Behr is funded by St George's Hospital Charity, RES 19-20002 'Genomics in Sudden Cardiac Death and Inherited Cardiac Conditions,' and supported by the Robert Lancaster Memorial Fund. Drs Sheppard and Westaby are supported by the charity, Cardiac Risk in the Young (CRY).

Disclosures

None.

Supplemental Material

Figures S1–S7

REFERENCES

1. Wu C-H, Chung P-I, Wu C-Y, Chen Y-T, Chiu Y-W, Chang Y-T, Liu H-N. Comorbid autoimmune diseases in patients with sarcoidosis: a nationwide case-control study in Taiwan. *J Dermatol*. 2017;44:423–430. doi: 10.1111/1346-8138.13654
2. Arkema EV, Grunewald J, Kullberg S, Eklund A, Askling J. Sarcoidosis incidence and prevalence: a nationwide register-based assessment in Sweden. *Eur Respir J*. 2016;48:1690–1699. doi: 10.1183/13993003.00477-2016
3. Arkema EV, Cozier YC. Epidemiology of sarcoidosis: current findings and future directions. *Thor Adv Chronic Dis*. 2018;9:227–240. doi: 10.1177/2040622318790197
4. Schupp JC, Freitag-Wolf S, Bargagli E, Mihailović-Vučinić V, Rottoli P, Grubanovic A, Müller A, Jochens A, Tittmann L, Schnerch J, et al. Phenotypes of organ involvement in sarcoidosis. *Eur Respir J*. 2018;51:51. doi: 10.1183/13993003.00991-2017
5. Iwai K, Tachibana T, Takemura T, Matsui Y, Kitaichi M, Kawabata Y. Pathological studies on sarcoidosis autopsy. I. Epidemiological features of 320 cases in Japan. *Acta Pathol Jpn*. 1993;43:372–376.
6. Sayah DM, Bradfield JS, Moriarty JM, Belperio JA, Lynch JP. Cardiac involvement in sarcoidosis: evolving concepts in diagnosis and treatment. *Semin Respir Crit Care Med*. 2017;38:477–498. doi: 10.1055/s-0037-1602381
7. Trivieri MG, Spagnolo P, Birnie D, Liu P, Drake W, Kovacic JC, Baughman R, Fayad ZA, Judson MA. Challenges in cardiac and pulmonary sarcoidosis: JACC state-of-the-art review. *J Am Coll Cardiol*. 2020;76:1878–1901. doi: 10.1016/j.jacc.2020.08.042
8. Gasperetti A, Rossi VA, Chiodini A, Casella M, Costa S, Akdis D, Büchel R, Deliniere A, Pruvot E, Gruner C, et al. Differentiating hereditary arrhythmogenic right ventricular cardiomyopathy from cardiac sarcoidosis fulfilling 2010 ARVC task force criteria. *Heart Rhythm*. 2021;18:231–238. doi: 10.1016/j.hrthm.2020.09.015
9. Asimaki A, Tandri H, Duffy ER, Winterfield JR, Mackey-Bojack S, Picken MM, Cooper LT, Wilber DJ, Marcus FI, Basso C, et al. Altered desmosomal proteins in granulomatous myocarditis and potential pathogenic links to arrhythmogenic right ventricular cardiomyopathy. *Circ Arrhythm Electrophysiol*. 2011;4:743–752. doi: 10.1161/CIRCEP.111.964890
10. Noorman M, Hakim S, Kessler E, Groeneweg JA, Cox MGPJ, Asimaki A, van Rijen HVM, van Stuijvenberg L, Chkourko H, van der Heyden MAG, et al. Remodeling of the cardiac sodium channel, connexin43, and plakoglobin at the intercalated disk in patients with arrhythmogenic cardiomyopathy. *Heart Rhythm*. 2013;10:412–419. doi: 10.1016/j.hrthm.2012.11.018
11. Chelko SP, Asimaki A, Lowenthal J, Bueno-Beti C, Bedja D, Scalco A, Amat-Alarcon N, Andersen P, Judge DP, Tung L, et al. Therapeutic modulation of the immune response in arrhythmogenic cardiomyopathy. *Circulation*. 2019;140:1491–1505. doi: 10.1161/CIRCULATIONAHA.119.040676
12. Baughman RP, Judson MA, Wells A. The indications for the treatment of sarcoidosis: Wells law. *Sarcoidosis Vasc Diffuse Lung Dis*. 2017;34:280–282.
13. Iannuzzi MC, Fontana JR. Sarcoidosis: clinical presentation, immunopathogenesis, and therapeutics. *JAMA*. 2011;305:391–399. doi: 10.1001/jama.2011.10
14. Besnard V, Jeny F. Models contribution to the understanding of sarcoidosis pathogenesis: "are there good models of sarcoidosis?." *J Clin Med*. 2020;9:9. doi: 10.3390/jcm9082445

15. Linke M, Pham HTT, Katholnig K, Schnöller T, Miller A, Demel F, Schütz B, Rosner M, Kovacic B, Sukhbaatar N, et al. Chronic signaling via the metabolic checkpoint kinase mTORC1 induces macrophage granuloma formation and marks sarcoidosis progression. *Nat Immunol*. 2017;18:293–302. doi: 10.1038/ni.3655
16. Calender A, Lim CX, Weichhart T, Buisson A, Besnard V, Rollat-Farnier PA, Bardel C, Roy P, Cottin V, Devouassoux G, et al. Exome sequencing and pathogenicity-network analysis of five French families implicate mTOR signalling and autophagy in familial sarcoidosis. *Eur Respir J*. 2019;54:1900430. doi: 10.1183/13993003.00430-2019
17. Hernandez O, Way S, McKenna J, Gambello MJ. Generation of a conditional disruption of the Tsc2 gene. *Genesis*. 2007;45:101–106. doi: 10.1002/dvg.20271
18. Caton ML, Smith-Raska MR, Reizis B. Notch-RBP-J signaling controls the homeostasis of CD8⁺ dendritic cells in the spleen. *J Exp Med*. 2007;204:1653–1664. doi: 10.1084/jem.20062648
19. Vogel B, Siebert H, Hofmann U, Frantz S. Determination of collagen content within picosirius red stained paraffin-embedded tissue sections using fluorescence microscopy. *MethodsX*. 2015;2:124–134. doi: 10.1016/j.mex.2015.02.007
20. Osmanagic-Myers S, Kiss A, Manakanatas C, Hamza O, Sedlmayer F, Szabo PL, Fischer I, Fichtinger P, Podesser BK, Eriksson M, et al. Endothelial progerin expression causes cardiovascular pathology through an impaired mechanoresponse. *J Clin Invest*. 2019;129:531–545. doi: 10.1172/JCI121297
21. Roberts WC, McAllister HA, Ferrans VJ. Sarcoidosis of the heart. A clinicopathologic study of 35 necropsy patients (group 1) and review of 78 previously described necropsy patients (group 11). *Am J Med*. 1977;63:86–108. doi: 10.1016/0002-9343(77)90121-8
22. Culver DA, Judson MA. New advances in the management of pulmonary sarcoidosis. *BMJ*. 2019;367:l5553. doi: 10.1136/bmj.l5553
23. Desai R, Kakumani K, Fong HK, Shah B, Zahid D, Zalavadia D, Doshi R, Goyal H. The burden of cardiac arrhythmias in sarcoidosis: a population-based inpatient analysis. *Ann Transl Med*. 2018;6:330. doi: 10.21037/atm.2018.07.33
24. Locke AH, Gurin MI, Sabe M, Hauser TH, Zimetbaum P. Arrhythmia in cardiac sarcoidosis. *Cardiol Rev*. 2021;29:131–142. doi: 10.1097/CRD.0000000000000354
25. Pendela VS, Kudaravalli P, Feitell S, Parikh V. Cardiac sarcoidosis masquerading as arrhythmogenic right ventricular cardiomyopathy: a case report. *Eur Heart J Case Rep*. 2021;5:ytab072. doi: 10.1093/ehjcr/ytab072
26. Munkholm J, Andersen CB, Ottesen GL. Plakoglobin: a diagnostic marker of arrhythmogenic right ventricular cardiomyopathy in forensic pathology? *Forensic Sci Med Pathol*. 2015;11:47–52. doi: 10.1007/s12024-014-9644-6
27. VanNorstrand DW, Asimaki A, Rubinos C, Dolmatova E, Srinivas M, Tester DJ, Saffitz JE, Duffy HS, Ackerman MJ. Connexin43 mutation causes heterogeneous gap junction loss and sudden infant death. *Circulation*. 2012;125:474–481. doi: 10.1161/CIRCULATIONAHA.111.057224
28. Andreoli A, Ruf MT, Itin P, Pluschke G, Schmid P. Phosphorylation of the ribosomal protein S6, a marker of mTOR (mammalian target of rapamycin) pathway activation, is strongly increased in hypertrophic scars and keloids. *Br J Dermatol*. 2015;172:1415–1417. doi: 10.1111/bjd.13523
29. Tavora F, Cresswell N, Li L, Ripple M, Solomon C, Burke A. Comparison of necropsy findings in patients with sarcoidosis dying suddenly from cardiac sarcoidosis versus dying suddenly from other causes. *Am J Cardiol*. 2009;104:571–577. doi: 10.1016/j.amjcard.2009.03.068
30. Ise T, Hasegawa T, Morita Y, Yamada N, Funada A, Takahama H, Amaki M, Kanzaki H, Okamura H, Kamakura S, et al. Extensive late gadolinium enhancement on cardiovascular magnetic resonance predicts adverse outcomes and lack of improvement in LV function after steroid therapy in cardiac sarcoidosis. *Heart*. 2014;100:1165–1172. doi: 10.1136/heartjnl-2013-305187
31. Terasaki F, Kuwabara H, Takeda Y, Yamauchi Y, Fujita S, Nakamura T, Torii I, Hirose Y, Hoshiga M. Clinical features and histopathology of cardiac sarcoidosis with refractory heart failure: an autopsy case. *Intern Med*. 2019;58:3551–3555. doi: 10.2169/internalmedicine.3147-19
32. Markatis E, Afthinos A, Antonakis E, Papanikolaou IC. Cardiac sarcoidosis: diagnosis and management. *Rev Cardiovasc Med*. 2020;21:321–338. doi: 10.31083/j.rcm.2020.03.102
33. Gulati A, Jabbour A, Ismail TF, Guha K, Khwaja J, Raza S, Morarji K, Brown TDH, Ismail NA, Dweck MR, et al. Association of fibrosis with mortality and sudden cardiac death in patients with nonischemic dilated cardiomyopathy. *Jama*. 2013;309:896–908. doi: 10.1001/jama.2013.1363
34. Kurmann R, Mankad SV, Mankad R. Echocardiography in sarcoidosis. *Curr Cardiol Rep*. 2018;20:118. doi: 10.1007/s11886-018-1065-9
35. Chapelon-Abric C, de Zuttere D, Duhaut P, Veyssier P, Wechsler B, Huong DLT, de Gennes C, Papo T, Blétry O, Godeau P, et al. Cardiac sarcoidosis: a retrospective study of 41 cases. *Medicine (Baltimore)*. 2004;83:315–334. doi: 10.1097/01.md.0000145367.17934.75
36. Tsampasian V, Maart C, Vassiliou VS, Garg P. Mitral valve disease in sarcoidosis diagnosed by cardiovascular magnetic resonance. *Lancet*. 2021;398:1358. doi: 10.1016/S0140-6736(21)01791-8
37. Lynch JP, Hwang J, Bradfield J, Fishbein M, Shivkumar K, Tung R. Cardiac involvement in sarcoidosis: evolving concepts in diagnosis and treatment. *Semin Respir Crit Care Med*. 2014;35:372–390. doi: 10.1055/s-0034-1376889
38. Damsky W, Thakral D, Emeagwali N, Galan A, King B. Tofacitinib treatment and molecular analysis of cutaneous sarcoidosis. *N Engl J Med*. 2018;379:2540–2546. doi: 10.1056/NEJMoa1805958
39. Krausgruber T, Redl A, Barreca D, Doberer K, Romanovskaia D, Dobnikar L, Guarini M, Unterluggauer L, Kleissl L, Aitzmüller D, et al. Single-cell and spatial transcriptomics reveal aberrant lymphoid developmental programs driving granuloma formation. *Immunity*. 2023;56:289–306.e7. doi: 10.1016/j.immuni.2023.01.014
40. Liu J, Ma P, Lai L, Villanueva A, Koenig A, Bean GR, Bowles DE, Glass C, Watson M, Lavine KJ, et al. Transcriptional and immune landscape of cardiac sarcoidosis. *Circ Res*. 2022;131:654–669. doi: 10.1161/CIRCRESAHA.121.320449
41. Houston BA, Mukherjee M. Cardiac sarcoidosis: clinical manifestations, imaging characteristics, and therapeutic approach. *Clin Med Insights Cardiol*. 2014;8:31–37. doi: 10.4137/CMC.S15713
42. Epelman S, Lavine KJ, Beaudin AE, Sojka DK, Carrero JA, Calderon B, Brijia T, Gautier EL, Ivanov S, Satpathy AT, et al. Embryonic and adult-derived resident cardiac macrophages are maintained through distinct mechanisms at steady state and during inflammation. *Immunity*. 2014;40:91–104. doi: 10.1016/j.immuni.2013.11.019
43. Bajpai G, Schneider C, Wong N, Bredemeyer A, Hulsmans M, Nahrendorf M, Epelman S, Kreisler D, Liu Y, Itoh A, et al. The human heart contains distinct macrophage subsets with divergent origins and functions. *Nat Med*. 2018;24:1234–1245. doi: 10.1038/s41591-018-0059-x
44. Bueno-Beti C, Asimaki A. Histopathological features and protein markers of arrhythmogenic cardiomyopathy. *Front Cardiovasc Med*. 2021;8:746321. doi: 10.3389/fcvm.2021.746321
45. Dan HC, Cooper MJ, Cogswell PC, Duncan JA, Ting JP-Y, Baldwin AS. Akt-dependent regulation of NF- κ B is controlled by mTOR and raptor in association with IKK. *Genes Dev*. 2008;22:1490–1500. doi: 10.1101/gad.1662308
46. Dai J, Jiang C, Chen H, Chai Y. Rapamycin attenuates high glucose-induced inflammation through modulation of mTOR/NF- κ B pathways in macrophages. *Front Pharmacol*. 2019;10:1292. doi: 10.3389/fphar.2019.01292
47. Manzia TM, Bellini MI, Corona L, Toti L, Fratoni S, Cillis A, Orlando G, Tisone G. Successful treatment of systemic de novo sarcoidosis with cyclosporine discontinuation and provision of rapamune after liver transplantation. *Transpl Int*. 2011;24:e69–e70. doi: 10.1111/j.1432-2277.2011.01256.x
48. Gupta N, Bleesing JH, McCormack FX. Successful response to treatment with sirolimus in pulmonary sarcoidosis. *Am J Respir Crit Care Med*. 2020;202:e119–e120. doi: 10.1164/rccm.202004-0914IM
49. Han Q, Lin L, Zhao B, Wang N, Liu X. Inhibition of mTOR ameliorates bleomycin-induced pulmonary fibrosis by regulating epithelial-mesenchymal transition. *Biochem Biophys Res Commun*. 2018;500:839–845. doi: 10.1016/j.bbrc.2018.04.148
50. Hettiarachchi SU, Li Y-H, Roy J, Zhang F, Puchulu-Campanella E, Lindeman SD, Srinivasarao M, Tsoyi K, Liang X, Ayoub EA, et al. Targeted inhibition of PI3 kinase/mTOR specifically in fibrotic lung fibroblasts suppresses pulmonary fibrosis in experimental models. *Sci Transl Med*. 2020;12:12. doi: 10.1126/scitranslmed.aay3724